JOURNAL OF THERMOPHYSICS AND HEAT TRANSFER
Vol. 15, No. 4, October–December 2001

Investigation on the Effects of Body Force Environment on Flat Heat Pipes

M. C. Zaghdoudi*
ATHERM, 38420 Domène, France
and
C. Sarno†
Sextant Avionique, 26027 Valence, France

This paper reports on the effects of body forces environment: gravitation, vibration, and acceleration forces using constant heat load on the thermal performance of a flat copper/water heat pipe. The effect of gravitation forces is studied by testing the heat pipe in different positions: horizontal, vertical with a heat source upwards (antigravity position), and vertical with a heat source downward (thermosyphon position). Transient accelerations and vibrations are generated using centrifuge and shaking tables, respectively, in order to simulate vibration and acceleration forces corresponding to aircraft maneuvering in frequency, amplitude, duration, and direction. The experimental results on the orientation effects show that the heat pipe is hardly affected by the gravitation forces and exhibits nearly the same thermal performance whatever the tilt angle for input heat powers lower than 20 W. For input heat powers higher than 20 W, there is a slight heat pipe thermal performance dependency on gravitation. For the vibration tests the heat pipe is mounted on a tri-axis shaking table and it is subjected to sinusoidal excitation. The heat-pipe thermal performance is hardly affected by vibration whatever the mounting direction on the shaking table. An investigation into the effects of transient acceleration forces with constant input heat loads on the heat-pipe thermal performance has been conducted. Pooling of the excess working fluid plays a significant role in the heat transport potential of the heat pipe subjected to accelerations. There is a decrease in the heat-pipe thermal performance with increasing acceleration as a result of partial dryout of the evaporator and pooling in the condenser section. Dryout, which is demonstrated as a result of increased acceleration, depends on the input heat power and the acceleration type. However, under certain acceleration tests the heat pipe successfully reprimed with a suppression of acceleration. In all cases the increase of the heat-pipe thermal resistance does not exceed 70%. The maximum heat-pipe thermal resistance obtained under 10-*g* acceleration level remains an acceptable value for the electronic package safety.

Nomenclature

F_v	=	vapor friction coefficient, s/m^4
F_l	=	liquid friction coefficient, s/m^4
g	=	gravitational acceleration, m/s^2
L_{eff}	=	effective length, m
Q	=	input heat power, W
$Q_{\max}$	=	maximum capillary heat flux rate, W
R_{th}	=	thermal resistance, K/W
r	=	radial location of accelerometer axis, m
T_{ev}	=	evaporator temperature, °C
T_c	=	condenser temperature, °C
γ	=	radial acceleration, m/s^2
$\Delta P_{c\,\text{eff}}$	=	effective capillary pressure, N/m^2
$\Delta P_{c\,\max}$	=	maximum capillary pressure, N/m^2
ΔP_v	=	vapor pressure drop, N/m^2
ΔP_γ	=	acceleration pressure drop, N/m^2
ΔP_l	=	liquid pressure drop, N/m^2
ω	=	angular velocity, rad/s

Introduction

PACKAGING and thermal management of electronic equipment have become an important problem because of increased power levels and simultaneous miniaturization of the devices. This may cause difficulties to use the latest packaging technologies available particularly in avionics or space applications. Indeed, more functions are being levied on aircraft systems. The raise of functional density increases the electronic component density. To meet the added functional requirements, electronic devices must shrink to allow more devices on a module and to allow the increase of processing/interconnection speeds. This, however, produces 1) an increase of card and module total heat dissipation so that the heat dissipated is greater than 100 W for a module and 2) an increase of local heat densities for highly integrated components so that heat fluxes underneath the chips could be higher than 25 W/cm^2.

The typical cooling techniques for avionics are based on cooling with conduction and with forced or natural convection. These techniques may provide no convenient source of cooling to prevent the electronics from operating at temperatures surpassing those required for maximum component life. New cooling techniques will have to be developed to maintain components within the temperature limits.

Heat-pipe technology may be able to provide sufficient cooling in these types of situations. Heat pipes have traditionally been operated in environments free of adverse body forces such as vibrations and high acceleration forces. Recently, heat pipes have been proposed to be used aboard fighter aircraft to act as heat sinks for electronic packages. During combat, transient acceleration fields up to 10 *g* could be present on the aircraft. Acceleration force fields may be transient and coupled with transient heat loads. Therefore, characterizing the steady state and transient performance of heat pipes under elevated acceleration fields is of importance to designers of the electronics packages in need of cooling and will require experimental approaches. Acceleration values should be obtained from the aircraft structural loads analyses. Figure 1 shows the six acceleration directions to which the aircraft can be submitted during maneuvering and combat. Suggested acceleration levels for different avionics

Received 17 July 2000; revision received 3 January 2001; accepted for publication 17 April 2001.

*Heat Pipe Research and Development Division, 1, Rue Charles Morel; currently Assistant Professor, Institute of Applied Sciences and Technology, Centre Urbain Nord, BP 676, 1080 Tunis, Tunisia; c.zaghdoudi@atherm.com. Member AIAA.

†Head of Packaging Design Office, Industrial Systems Department, 25, Rue Jules Védrines.

Table 1 Suggested *g* levels for different avionics vehicles

		Test level					
		Direction of vehicle acceleration (Fig. 1)					
						Lateral	
Vehicle category	Forward acceleration A, *g*	Fore	Aft	Up	Down	Left	Right
Aircraft[a,b]	2	1A	3A	4.5A	1.5A	2A	2A
Helicopters[c]	——	2	2	7	3	4	4
Manned aerospace vehicles[d]	6 to 12	1A	0.33A	1.5A	0.5A	0.66A	0.66A

[a]For carrier-based aircraft the minimum value to be used for A is 4, representing a basic condition associated with catapult launches.
[b]For attack and fighter aircraft add pitch, yaw, and roll accelerations as applicable.
[c]For helicopters forward acceleration is unrelated to acceleration in other directions. Test levels are based on current and near future helicopter design requirements.
[d]When forward acceleration is not known, the high value of the acceleration range should be used.

Table 2 Overview of studies on acceleration effects on heat-pipe thermal performances

Authors	Study	Acceleration levels, *g*	Heat-pipe specifications	Fluids
Kiseev et al.[1]	Experimental	5 and 10	Axially grooved	Acetone Freon 11 n-pentane ammonia
Ponnappan et al.[2]	Experimental	Up to 10	Flexible	Water
Yerkes and Beam[3]	Experimental	Up to 10	Flexible/arterial	Water
Peng et al.[4]	Analytical	——	Arterial	Water
Ochterbeck et al.[5]	Theoretical	——	Arterial	Water
	Experimental	——	Arterial	Water
Thomas and Yerkes[6]	Experimental	Up to 10	Flexible	Water
Romestant and Alexander[7]	Experimental	Up to 10	Axially grooved	Ammonia
			Sintered powder	Water
Thomas et al.[8]	Experimental	Up to 10	Helically grooves	Ethanol
			Straight grooves	

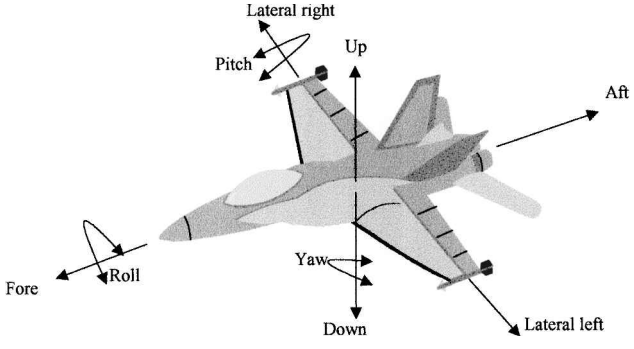

Fig. 1 Acceleration directions during maneuvering and combat.

vehicles are presented in Table 1 (standard military specifications: MIL-STD-810D—Procedure II: operational test).

Moreover, vibrations cannot be avoided in the aircraft equipment. Therefore, some study of the effects of vibrations on the performance of heat pipes must be carried out to determine if vibrations will either aid or hinder the operation of the heat pipe.

Gravitational forces have long been used to return the condensate to the evaporator section of thermosyphons. However, investigations concerning the analysis of the performance of heat pipes subjected to steady state and transient acceleration forces greater than 1-*g* environment are scarce. Investigations on the heat-pipe performance with the inclusion of acceleration forces are typically done to verify wicking properties for specific wick structures. These investigations have included 1) dryout and rewetting phenomena under axial acceleration with constant heat load, 2) dryout and rewetting phenomena under axial and transverse acceleration with step changes in heat load, and 3) dryout and rewetting phenomena under accelerations induced by direction changes with constant heat load. Studies on acceleration effects on heat pipes are summarized in Table 2.

Kiseev et al.[1] experimentally investigated the performance of an antigravity heat pipe with separate liquid and vapor channels subjected to acceleration forces of 1, 5, and 10 *g*. The heat pipes were filled with acetone, pentane, and Freon 11 as working fluids. They found that the heat pipe operated with a reduced maximum heat flux accompanied by a large thermal resistance when subjected to adverse acceleration forces. A Bond number for the heat pipe was derived as a balance between the pressure exerted on the fluid caused by acceleration and the available capillary pressure caused by the surface tension

$$Bo = \frac{\rho \gamma L d_p \sin\phi}{4\sigma \cos\theta}$$

where L is the length of the heat transfer section of the antigravity heat pipe, ϕ is the tilt angle of the heat pipe with respect to horizontal, d_p is the average pore diameter, and θ is the wetting angle. It was determined that the heat pipe operation stops when the Bond number is greater than unity.

Ponnappan et al.[2] studied the effects of acceleration on a flexible copper-water arterial heat pipe by using centrifuge table. Different possible mounting orientations were considered so that radial and tangential accelerations, which are favorable and unfavorable for liquid return, were applied. Like the Kiseev study, a Bond number is defined as follows:

$$Bo = \gamma(\rho_1 - \rho_v) d_a r_c / \sigma$$

where d_a is the diameter of the artery, r_c is the capillary pore radius, and σ is the surface tension. In a circumferentially mounted orientation it was found that the flexible heat pipe operated safely for radial accelerations of up to 10 *g*. For a radially mounted orientation and steady-state accelerations of 1.01, 2.35, 4.35, and 10.1 *g*, it was found that the dryout limit decreases with increasing radial acceleration (Fig. 2) because of the depriming of the artery. As the heat load is reduced, however, the artery is able to reprime.

Yerkes and Beam[3] reported the effects of transient and axial acceleration forces with step changes in input power on the performance of a flexible copper/water arterial heat pipe. Heat-pipe performance as a result of transient transverse acceleration forces from 1 to 10 *g*

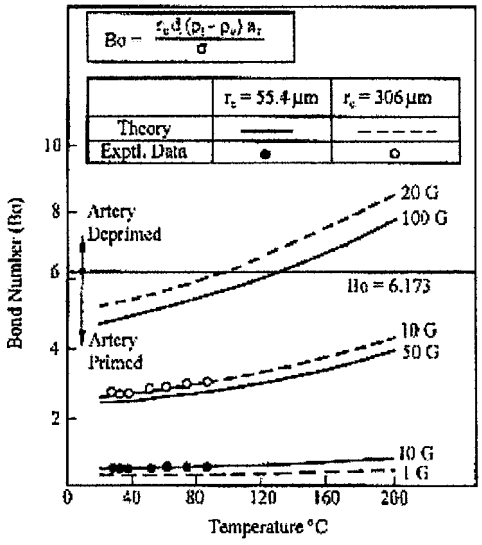

Fig. 2 Effect of radial acceleration on heat-pipe performance.[2]

in the form of step changes, sinusoidally varying steady periodic cycles, and burst cycles were presented. The burst cycles consisted of a sinusoidal radial acceleration, followed by a steady-state acceleration of 2 *g*, where each component lasted for 5 min. Partial depriming of the artery, pooling of the unconstrained working fluid, and fluid sloshing were found to have a significant impact on the heat transport and the transient behavior of the heat pipe. Repriming of the heat pipe under thermal load while being subjected to transient transverse accelerations was also demonstrated.

Peng and Peterson[4] conducted an analytical investigation to determine the effect of short-term longitudinal accelerations on the liquid-vapor interface in external artery heat pipes, which have been suggested for use as external radiator elements on Space Station *Freedom.* Changes in orbital attitude or docking maneuvers impose longitudinal accelerations, which may force the liquid in the channel into the vapor channel, thereby depriming the heat pipe. Closed-form expressions for the locations of the liquid-vapor interfaces in the liquid channel, the vapor channel, and the slot connecting them were derived as functions of time. Also, the steady locations under a constant acceleration were determined. The lengths of the liquid columns in the liquid and vapor spaces were functions of time, the acceleration magnitude, the working fluid properties, and the internal geometry of the heat pipe.

Ochterbeck et al.[5] developed a combined analytical and numerical model in order to analyze the deprime and reprime/rewetting characteristics of arterial heat pipes undergoing induced accelerations. The results of the theoretical analysis were then compared with the experimental results obtained from acceleration tests conducted aboard STS-43. The depriming analysis indicated the importance of frictional effects on the liquid configuration during an external acceleration. In addition, the evaporator recovery time of the heat pipe was found to be dominated by the liquid artery reprime/rewetting characteristics as opposed to the characteristics of the circumferential wall grooves.

Thomas and Yerkes[6] determined the quasi-steady-state thermal resistance of a flexible copper/water heat pipe under transient acceleration fields with constant heat input. The performance of the heat pipe was examined in terms of the heat input, condenser temperature, radial acceleration, and sinusoidal acceleration frequency. In addition, the effects of the previous dryout history were noted. It was found that the thermal resistance of the heat pipe decreased with increasing acceleration frequency and condenser temperature and increased with the heat input.

Romestant and Alexander[7] studied the effect of the axial acceleration variations caused by direction changes typifying high-performance aircraft maneuvering on two types of commercially available heat pipes: aluminum/ammonia axially grooved heat pipes and copper/water sintered powder heat pipes. It was demonstrated that both heat pipes are sensitive to transient acceleration up to 6 *g* induced by rapid change in directions.

Thomas et al.[8] studied experimentally and theoretically the effects of transverse acceleration-induced body forces on the capillary limit of helically or straight grooved heat pipes with ethanol as working fluid. The heat pipe is mounted on the centrifuge table circumference so that uniform transverse acceleration could be applied along the entire length of the heat pipe. The heat pipe is mounted to a platform, which overhangs the edge of the horizontal centrifuge table. This allows the heat pipe to be positioned such that the radius of curvature is equivalent to the outermost radius of the centrifuge table. Therefore, the heat pipe has a circumferencial mounting orientation with a condenser leading end, which indicates that the acceleration actually aided in the return of the working fluid back to the evaporator section. By varying the heat input and centrifuge table velocity, information on dryout phenomena, thermal resistance, and the capillary limit was obtained. Because of the geometry of the helical grooves, the capillary limit increases by a factor of five when the radial acceleration increases from 0 to 6 *g*. The experimental study on the heat pipe with straight grooves showed that their thermal performance was not improved when radial acceleration was increased from 0 to 10 *g*.

Most of the experimental studies have been carried out in the absence of vibration, even though almost all heat-pipe applications involve vibrations.

Deverall[9] tested a stainless-steel/water heat pipe under sinusoidal and random vibrations. Three wraps of 100-mesh stainless-steel screen were used as the capillary wick. Heat input was achieved with a coiled heater rod, which was soldered to the heat pipe, and heat was released from the pipe by natural convection. Experimental parameter ranges were as follows: vibration frequency, 0–2000 Hz; acceleration, 0–12 *g*; inclination angle from horizontal, 0–40 deg; working temperature 60, 70, 90°C. At the maximum angle against gravity, the liquid drained out of the wick and puddled in the condenser section, leading to a temperature drop in that section of 7°C. When the vibrations were started, the heat pipe became isothermal to within 1°C. It was suggested by the author that the initial wetting of the wick after assembly of the heat pipe could be accelerated by applying vibrations.

Richardson et al.[10] carried out experiments on the effect of longitudinal vibration on a long stainless-steel/water heat pipe. The frequency of vibrations ranged from 0 to 580 Hz, the acceleration from 0 to 12 *g*, and the inclination angle against gravity was 32, 35, and 38 deg. It was determined that longitudinal vibrations decrease the maximum heat-transport capacity of the heat pipe. This decrease was found to be more severe at lower frequencies and higher acceleration levels.

The results of the previous studies have indicated a need for improved thermal performance under acceleration fields and vibrations. In addition, a capillary wick is sought to provide an adequate behavior of the working fluid within heat pipes under these conditions. Therefore, to address these points a heat pipe with arteries and sintered powder is fabricated and tested. The objectives of this study are to examine the thermal behavior of a copper/water flat heat pipe under different tilt angles: horizontal, vertical with a heat source downwards (thermosyphon position), and vertical with a heat source upwards (antigravity position). Thermal performances are also determined when the heat pipe is subjected to sinusoidal vibrations and transient axial acceleration forces with step variations in amplitude and duration. Accelerations up to 10 *g* are applied for different input heat fluxes.

Theoretical Background

For a heat pipe to function properly, the net capillary pressure difference between evaporator (heat source) and condenser (heat sink) must be greater than the summation of all pressure losses occurring throughout the liquid and vapor flow paths. This relationship, referred to as the capillary limitation, can be expressed mathematically as

$$\Delta P_{c\max} \geq \Delta P_l + \Delta P_v + \Delta P_\gamma \qquad (1)$$

In this relation pressure drop across phase transition in evaporator and condenser are neglected. One can note that if $\gamma = 1\ g$, ΔP_γ represents hydrostatic pressure drop. When the maximum capillary pressure is equal to or greater than the summation of these pressure drops, the capillary structure is capable of returning an adequate amount of working fluid (priming or repriming of the heat pipe) to prevent dryout of the evaporator wicking structure. When the summation of all pressure drops exceeds the maximum capillary pumping pressure, the working fluid is not supplied rapidly enough to the evaporator to compensate for the liquid loss through vaporization and the wicking structure becomes starved of liquid and dries out (depriming of the heat pipe). This condition referred to as capillary limitation varies according to the wicking structure, working fluid, evaporator heat flux, operating temperature, and body forces.

The maximum capillary heat flux rate that can be transferred by a wicked heat pipe is

$$Q_{\max} = \frac{\Delta P_{c\max} - \Delta P_\gamma}{(F_1 + F_v)L_{\text{eff}}} = \frac{\Delta P_{c\,\text{eff}}}{(F_1 + F_v)L_{\text{eff}}} \tag{2}$$

where L_{eff} is equal to $L_a + 0.5\ (L_e + L_c)$. L_a, L_e, and L_c are the adiabatic, evaporator, and condenser lengths, respectively. These coefficients depend on the liquid and vapor flow regimes and the wick properties.[11,12]

Equation (2) shows that submitting a wicked heat pipe to adverse acceleration forces will reduce the effective capillary pressure and the maximum capillary heat flux rate. The accelerations as well as vibrations could result in redistribution of the working fluid and require a reduction in the evaporator heat flux to allow rewetting of the wick structure. This point is the subject of the present paper.

Heat-Pipe Structure and Test Rig

The purpose of the experiments is to examine the thermal performance of a sintered powder arterial flat copper/water heat pipe under various heat inputs, tilt angles, sinusoidal vibrations, and axial accelerations.

Heat Pipe and Wicking Structures

A flat heat pipe (FHP), designed especially for aircraft applications, is used for the experimental testing (Fig. 3a). The main characteristics of this heat pipe are given in Table 3. The FHP (Fig. 3b) is manufactured with an axial and rectangular capillary groove structure (0.7 mm wide and 1 mm deep) and a porous copper plate (30 mm wide, 115 mm length, and 1.9 mm thickness). The heat-pipe body is manufactured in two halves as shown in Fig. 3a. Manufacturing of FHP begins with the capillary grooves being mechanically machined in the first half. Sintered copper powder is fixed to the second half, which is machined for this purpose. The next step of the FHP manufacturing is to join the two halves by electronic beam welding. After testing the FHP for leaks (Helium test), the heat pipe is charged with 1.4 ml of water by a conventional boiling off method. The liquid charge is determined by the weighting method after the filling procedure is completed. Because the introduction of a determined optimum amount of water is difficult on these small scales, a sufficient fill criteria for the FHP is therefore defined as the fill ratio that produces a sufficiently small temperature drop in the condenser during normal heat-pipe operation, which signifies that the condenser is not blocked with excess liquid. Filling of the heat pipe with the optimum amount to properly work presents one of the greatest challenges of this study because the heat-pipe thermal behavior under acceleration fields depends greatly on this parameter.

Experimental Setup and Instrumentation

The heat pipe is mounted on a special setup (cooling system) in order to conduct experiments in acceleration conditions. The heat pipe is attached to an aluminum heat sink as illustrated in Fig. 4. Heat input is provided by a 40 × 15-mm thermofoil heater located at one end of the heat pipe, much like an electronic component would be in an actual application. Input power for the heater and airflow are supplied by precision power supplies through rotating contactors fixed inside the centrifuge table-rotating axis. The input power is calculated using the current and voltage readings. Steady-state variation in input heater power, caused by the voltage drop along the rotating contactors, is found to be ±2%. Heat is removed by an aluminum heat sink attached to the copper heat-pipe end opposite the heater. A thermally conductive paste is used to enhance the heat transfer between the heat pipe and the aluminum heat sink. The heat pipe is cooled by air, which is provided by a fan so that the aluminum heat sink is maintained at a constant temperature.

Three type-J surface mounted thermocouples are used to monitor the electrical heater, evaporator, and condenser temperatures. All of the thermocouples are mounted directly to the surface of the heat pipe. Mounting locations for the thermocouples are shown in Fig. 5.

Uncertainty Analysis

Uncertainty estimates for the heat input, heat transferred, and thermal resistance are given in this section. The heat input to the

Table 3 Heat-pipe specifications

General	Dimensions
Heat-pipe length	125 mm
Heat-pipe width	40 mm
Heat-pipe thickness	2.4 mm
Design power	60 W
Working fluid	Water
Wall/wick material	Copper
Capillary structure	Arteries and sintered powder
Total weight	75 g
Evaporator	
Length	15 mm
Width	40 mm
Condenser	
Length	15 mm
Width	40 mm

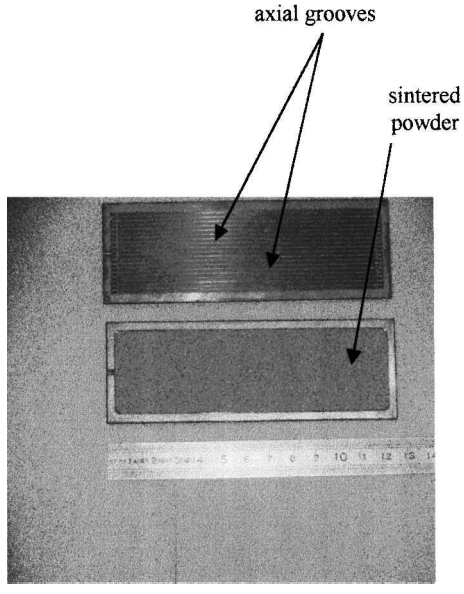

Fig. 3a FHP global view.

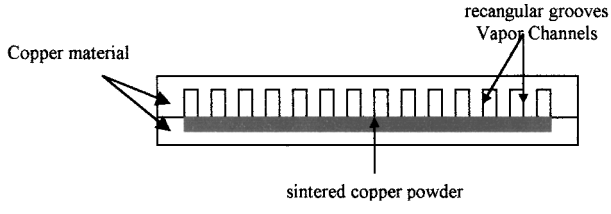

Fig. 3b Sketch of the FHP structure.

electric heater is calculated using the measured amperage and voltage ($Q = V \times I$). The thermal resistance R_{th} of the heat pipe is defined as the ratio of the temperature drop $T_{ev} - T_c$ across the heat pipe to the input heat power Q. Using the analysis given by Kline and McClintock,[13] the maximum rss uncertainties for all of the measured and calculated values presented in this paper are given in Table 4.

Experimental Methodology and Results

Effects of Gravitation on Heat-Pipe Thermal Performance

To determine the significance of the gravitational forces, experiments are carried out with different heat-pipe orientations (Fig. 6): horizontal position, favorable vertical position (thermosyphon position: the condenser is up and the evaporator is down), and the unfavorable vertical position (antigravity position: the condenser is down, and the evaporator is up).

A comparative technique is used to evaluate the steady-state and transient behavior of the heat pipe. In this technique the heat pipe and a copper plate having the same dimensions as the heat pipe are attached to a common aluminum heat sink. Heat input is provided by thermofoil heaters located at one end of the heat pipe and the copper plate surfaces. The heaters are connected in parallel to ensure that a constant power is supplied to each evaporator section.

Series of runs, in which the heat sink temperature is fixed at 30°C and the input power is varied incrementally, are carried out to determine the input power effect on the evaporator temperature. Figure 7a illustrates the source-sink temperature difference variations $T_{ev} - T_c$ as a function of the input heat flux rate Q obtained for the heat pipe and the copper plate. As it is shown, the heat-pipe source-sink temperature difference is significantly lower than that obtained for the copper plate. These results show the effectiveness of the heat pipe and clearly indicate the reduction level that can be expected at higher heat flux rates prior to dryout. Indeed, for a given input power, a threefold decrease in thermal resistance is obtained when using the heat pipe instead of a copper plate having the same dimensions. Moreover, input powers as high as 45 W can be reached without exceeding critical temperature on the thermofoil heater. However, when using the copper plate, the maximum allowable input power is 30 W for which a high thermofoil temperature exceeding 140°C is reached.

It is also noticed that the heat-pipe thermal performances are nearly independent of the orientation for input heat fluxes lower than 20 W. For input heat power higher than 20 W, the heat pipe exhibits thermal performance dependency on gravitation: the thermosyphon position gives the lowest heat source-heat sink difference. As it is noticed in Fig. 7a, the heat source-heat sink difference temperature gap between thermosyphon and antigravity positions increases with increasing heat flux rates. Indeed, this gap increases from 4 to 11°C for input powers ranging from 20 to 40 W. Figure 7b shows the

Table 4 Maximum uncertainties of measured and calculated values

Parameter	Value
Measured values	
Heater temperature	±1°C
Evaporator temperature	±1°C
Condenser temperature	±1°C
Heater voltage	±2% of reading
Heater current	±2% of reading
Radial acceleration	±0.1 *g*
Calculated values	
Heat input	±4%
Thermal resistance	±15%

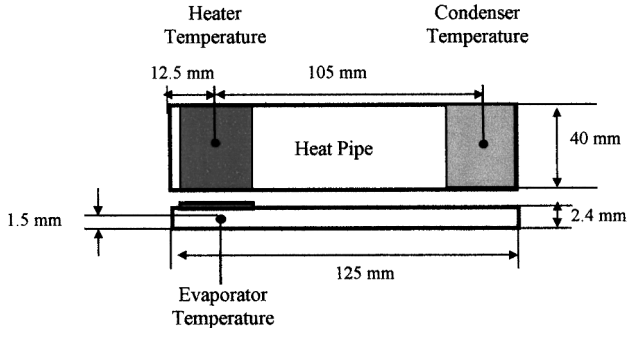

Fig. 5 Thermocouples location on the heat pipe.

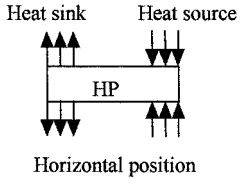

Fig. 6a Horizontal position.

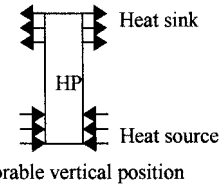

Fig. 6b Thermosyphon position.

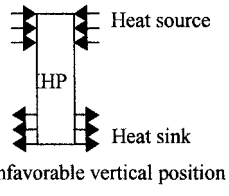

Fig. 6c Antigravity position.

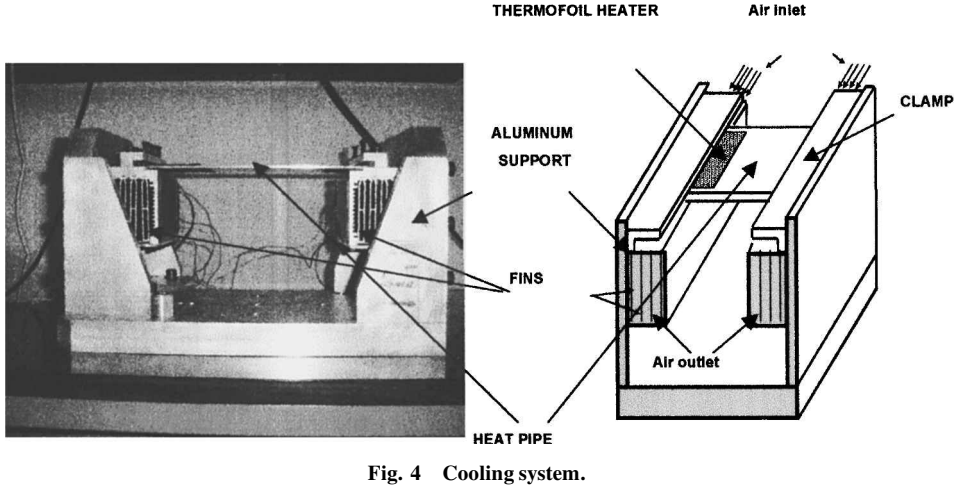

Fig. 4 Cooling system.

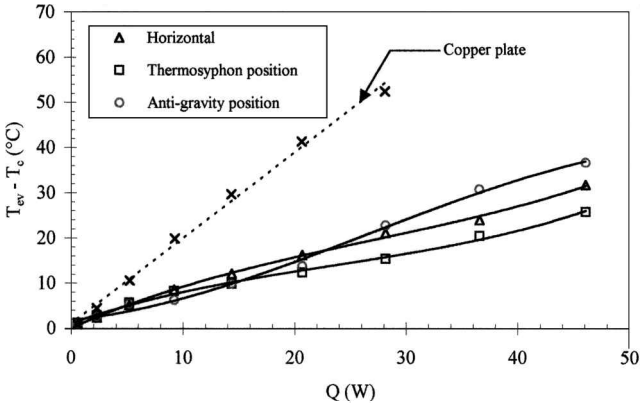

a) Evaporator-condenser temperature difference vs heat input rate

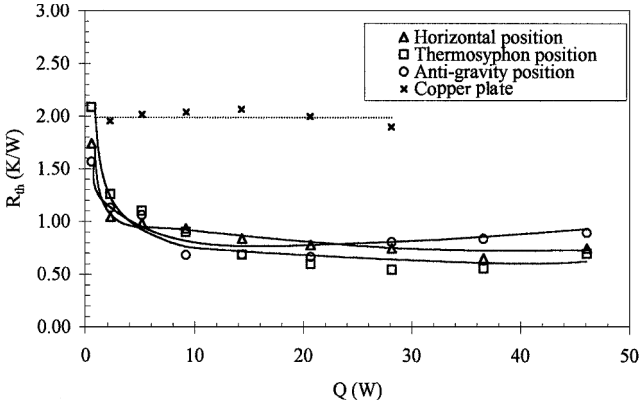

b) Thermal resistance vs heat input

Fig. 7 Effect of orientation on the heat-pipe thermal performance.

thermal resistance variations as a function of the input heat flux rates. The thermal resistance decreases with increasing input heat flux rates and then remains nearly constant for input powers higher than 20 W for the horizontal and the thermosyphon positions. However, for the antigravity position the heat-pipe thermal resistance increases when input powers exceed 20 W. The lowest thermal resistance is obtained for the thermosyphon position.

Vibration Effects on Heat-Pipe Thermal Performance

In the vibrations experiments the cooling system is placed on a shaking table. The vibration axis is that corresponding to the liquid flow inside the heat pipe. Sinusoidal vibrations are applied corresponding to the spectrum conditions: 50–2000 Hz (5 and 10 *g*, logarithmic sweep speed: 1 octave/min). The tests have been carried out for a heat input power of 30 W, and the heat pipe is horizontally oriented. Figure 8 shows the evaporator and condenser temperatures variations vs time for both acceleration levels (5 and 10 *g* in Figs. 8a and 8b, respectively). Thermal resistance and evaporator-condenser temperature variations are given in Figs. 9a and 9b.

For both acceleration levels the heat-pipe thermal resistance is slightly affected by vibrations. The evaporator and condenser temperatures as well as thermal resistance fluctuations are low. The average thermal resistance obtained under vibrations and for 30 W is 1 K/W, which is higher than that obtained during the static tests (see preceding section) in the same conditions, for example, in horizontal position (≈0.8 K/W).

Acceleration Effects on Heat-Pipe Thermal Performance

Acceleration forces are generated after mounting the already described setup on a centrifuge table (Fig. 10). Transient acceleration forces consisting of step changes are generated by controlling the angular velocity of the centrifuge table. An accelerometer is used to monitor the time-variant acceleration forces. For these experiments the heat pipe is mounted such that only axial accelerations are considered. Because the heat-pipe assembly is subjected to great

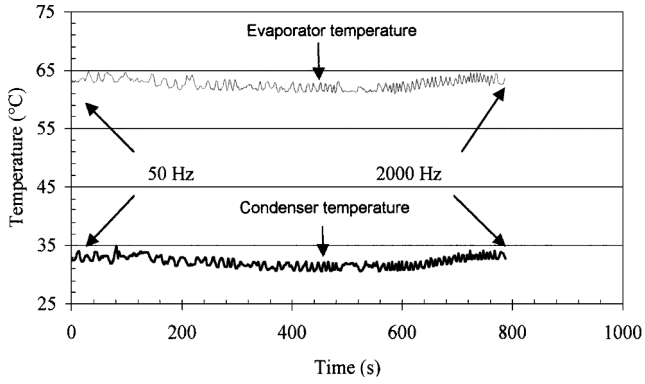

a) Temperature vs time (5 *g* sinus, Q = 30 W)

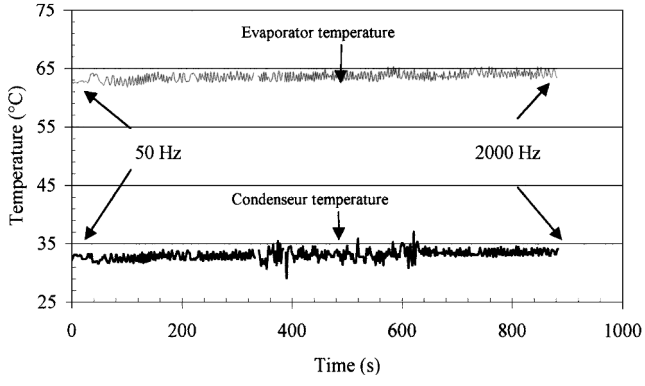

b) Temperature vs time (10 *g* sinus, Q = 30 W)

Fig. 8 Effect of vibrations on the heat-pipe thermal performance.

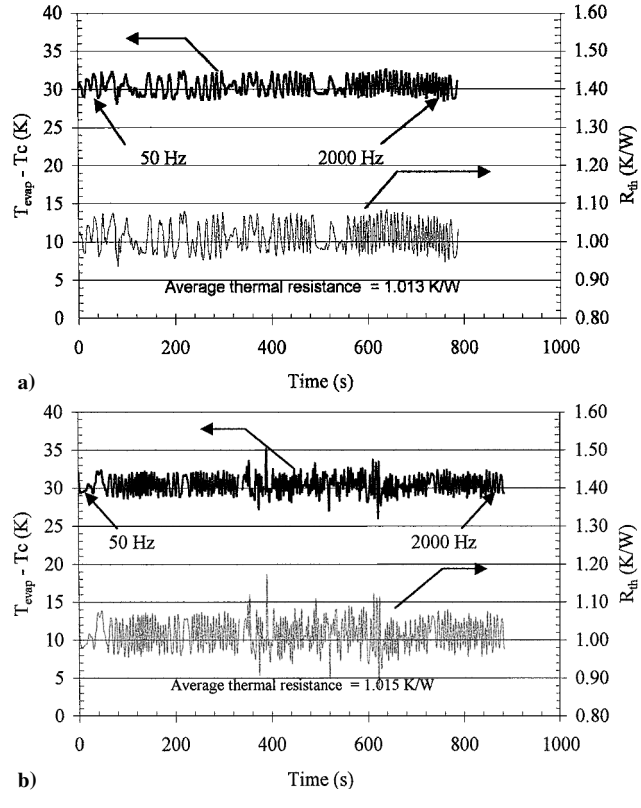

Fig. 9 Effect of vibrations on the heat-pipe thermal performance: a) evaporator-condenser temperature difference and R_{th} variations vs time (5 *g* sinus, Q = 30 W) and b) evaporator-condenser temperature difference and R_{th} variations vs time (10 *g* sinus, Q = 30 W).

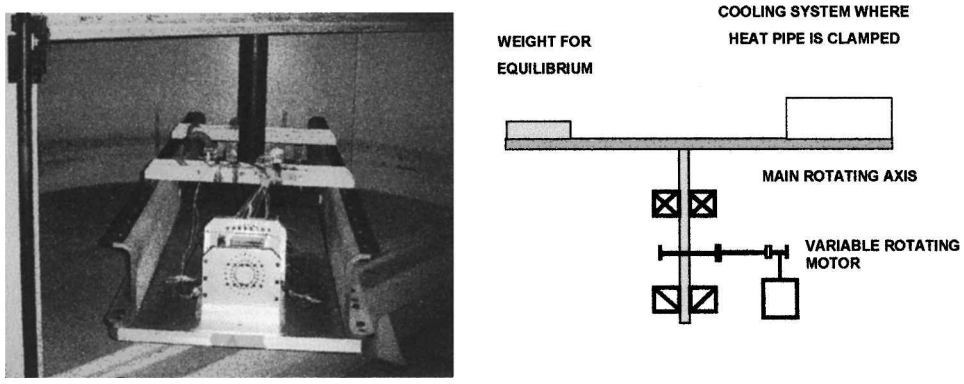

Fig. 10 Experimental setup for acceleration tests.

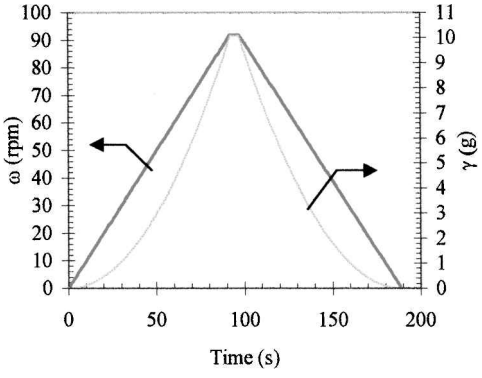

Fig. 11 Acceleration profiles (type 1).

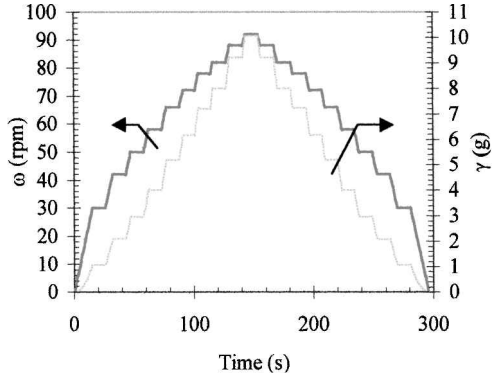

Fig. 12 Acceleration profiles (type 2).

air velocities caused by the rotation of the table, the entire heat pipe is insulated in order to reduce convective heat losses from the exterior of the heat pipe and to provide a reasonable adiabatic operating environment. Heat losses are estimated to be less than 2% of the input heat power. The output thermocouple signals are amplified and linearized to 0–10 V signal on the centrifuge table prior to data acquisition through the rotating contactors. Conditioning the temperature signals prior to leaving the centrifuge table avoids the disturbance of the thermocouple signal by the voltage drop in the rotating contactors.

Three types of accelerations are considered in this study. The first type (type 1) of acceleration is generated using a time-variant centrifuge table angular velocity ω in the form of linear curve. The slope of this curve, which represents the speed of the centrifuge table angular velocity increase or decrease, can be varied so that the duration of the applied acceleration can be modified. In this study the speed, at which the centrifuge table angular velocity is increased or decreased, is fixed at 1 rpm/s. This results in the centrifuge table angular velocity and acceleration profiles depicted in Fig. 11. The acceleration profile is parabolic because it is related to the angular velocity by $\gamma = \omega^2 r$. Hence, a centrifuge table angular velocity up to 94 rpm, which corresponds to a radial acceleration level of about 10 g, is reached in 94 s. This duration corresponds to the acceleration increase and decrease time and a 5-s stabilization for the 10-g acceleration level.

The second type (type 2) is generated using a step change in the centrifuge table angular velocity ω. The speed, at which the centrifuge table angular velocity is increased or decreased, is fixed at 1 rpm/s. This results in the centrifuge table angular velocity and acceleration profiles depicted in Fig. 12. A stabilization of 10 s is considered for each acceleration level. The overall duration of this test is about 300 s, and 10-g acceleration level is reached in 140 s.

The third type of acceleration (type 3) test consists of increasing and decreasing the acceleration level after thermal stabilization. This test is the longest one because it depends on the time needed to reach the steady-state heat-pipe operation for each acceleration level.

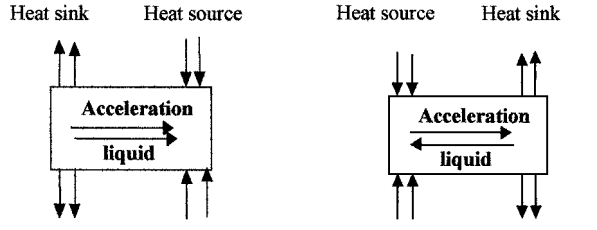

a) Favorable position b) Unfavorable Favorable position

Fig. 13 Heat-pipe mounting on the cooling system.

The experiments are carried out for different constant heat loads, and the preceding acceleration types are applied for each heat load level. The heat pipe is mounted on the centrifuge table in such a way that acceleration forces are opposite to the liquid flow (unfavorable heat-pipe mounting, Fig. 13b).

Heat-Pipe Behavior Under Acceleration Forces of Type 1

For this type of acceleration, heat-pipe temperatures for the heater, evaporator, and condenser are plotted with time for different input powers ($Q = 20$, 30, and 40 W) in Fig. 14. With steady-state input powers of 20 W (Fig. 14a), 30 W (Fig. 14b), and 40 W (Fig. 14c), the acceleration initiating dryout is approximately 6, 4, and 3 g, respectively. These acceleration levels correspond to a sharp increase of the temperatures (evaporator and heater temperatures). Dashed lines are reported on the curves in order to indicate these levels. The heat-pipe thermal resistance R_{th} variations as a function of time are depicted in Fig. 15. In zero acceleration field the heat-pipe thermal resistance decreases with increasing input heat loads and increases when approaching dryout ($R_{th} \approx 0.75$ K/W for $Q = 20$ W, $R_{th} \approx 0.56$ K/W for $Q = 30$ W and $R_{th} \approx 0.68$ K/W for $Q = 40$ W). In acceleration field, for $Q = 20$ W, the increase in the heat-pipe thermal resistance is about 20% for 10 g (Fig. 15a). For $Q = 30$ W and 40 W (Figs. 15b and 15c) the increase in R_{th} is about 60 and 70%, respectively, for the same acceleration level. For $Q = 20$ W the heat pipe is not reprimed

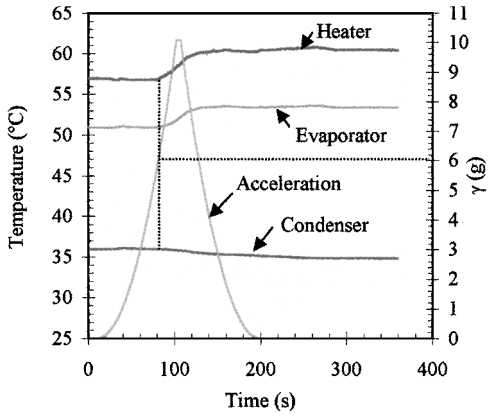

a) Q = 20 W

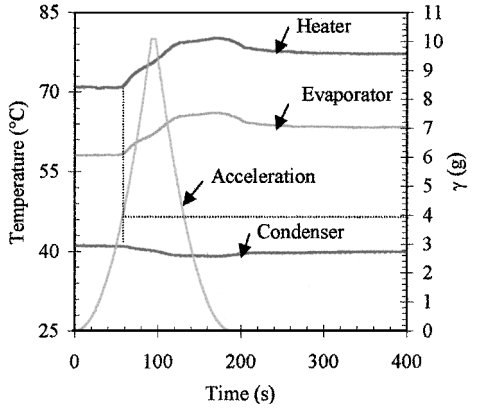

b) Q = 30 W

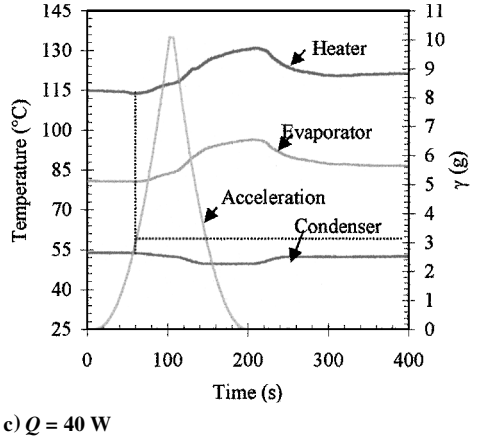

c) Q = 40 W

Fig. 14 Temperature variations vs time (acceleration of type 1).

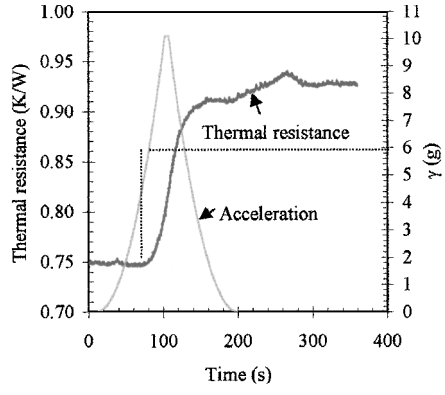

a) Q = 20 W

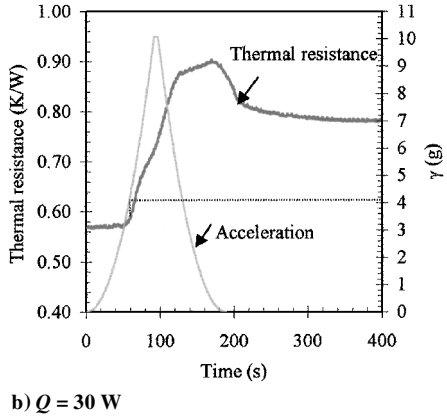

b) Q = 30 W

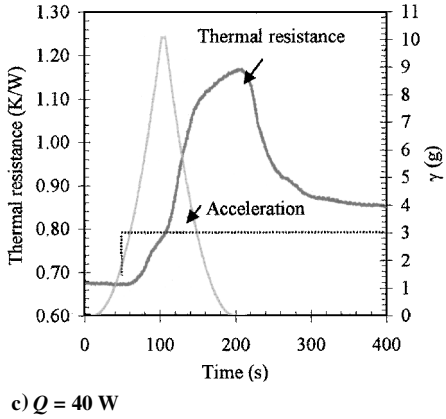

c) Q = 40 W

Fig. 15 Thermal resistance variations vs time (acceleration of type 1).

although the acceleration is suppressed. For $Q = 30$ W there is a partial repriming of the heat pipe, and for $Q = 40$ W a nearly complete repriming of the heat pipe is accomplished. Hence, the transient behavior of the heat pipe under acceleration depends not only on the acceleration level but also on the input heat load. Dryout and depriming of the wick structure is caused by a combination of heat flux rate and acceleration.

Heat-Pipe Behavior Under Acceleration Forces of Type 2

Figure 16 shows experimental results for the heat pipe with steady-state input power and submitted to acceleration forces of type 2. Heat-pipe temperatures for the heater, evaporator, and condenser are plotted with time for input powers of 20 W (Fig. 16a) and 40 W (Fig. 16b). The heat-pipe thermal resistance variations as a function of time are depicted in Fig. 17. In acceleration field the heat-pipe thermal resistance increase is about 30% for $Q = 20$ W (Fig. 17a) and 40% for $Q = 40$ W (Fig. 17b) for 10-g acceleration level. The acceleration initiating dryout, which causes a sharp and rapid increase of the evaporator and heater temperatures as well as the heat-pipe thermal resistance, is approximately 5 g (indicated by dashes lines on the curves) for both input heat loads. As it is noticed for the preceding acceleration type, the heat pipe is not reprimed although the acceleration is suppressed for input heat load $Q = 20$ W. For $Q = 40$ W there is a total repriming of the heat pipe.

Heat-Pipe Behavior Under Acceleration Forces of Type 3

Temperature and acceleration data vs time for acceleration test run of type 3 are presented in Fig. 18 for two different heat input settings. In Fig. 18a, with a heat input of $Q = 20$ W, the transient behavior of the heat pipe is completely different from the preceding acceleration types (types 1 and 2). Indeed, repriming of the heat pipe is observed immediately after acceleration suppression. With heat input of $Q = 40$ W (Fig. 18b), the same transient behavior as in type 1 and 2 accelerations is noticed. However, this type of acceleration tends to shift or delay the onset of dryout. Indeed, the accelerations initiating dryout are approximately 7 and 5 g (indicated by dashed lines on the curves) for $Q = 20$ and 40 W, respectively. Thermal resistance and acceleration data vs time are depicted in Fig. 19. The increase in the heat-pipe thermal resistance is about 50% for

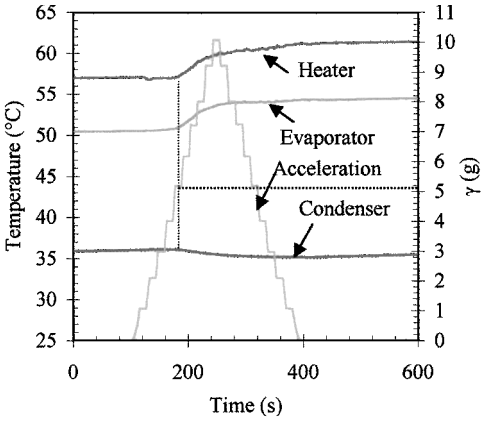

a) Q = 20 W

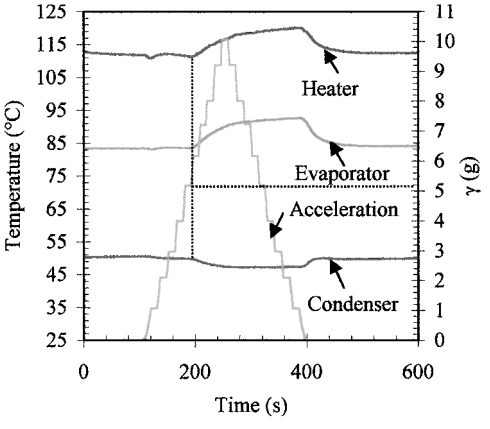

b) Q = 40 W

Fig. 16 Temperature variations vs time (acceleration of type 2).

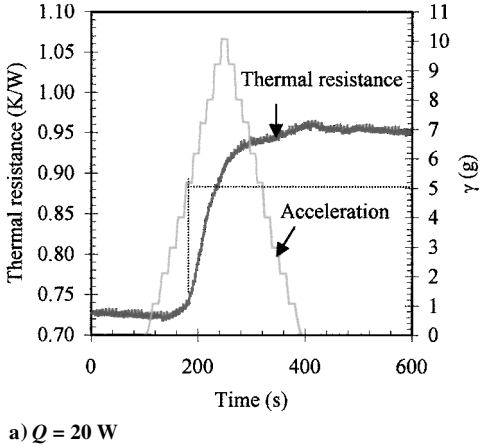

a) Q = 20 W

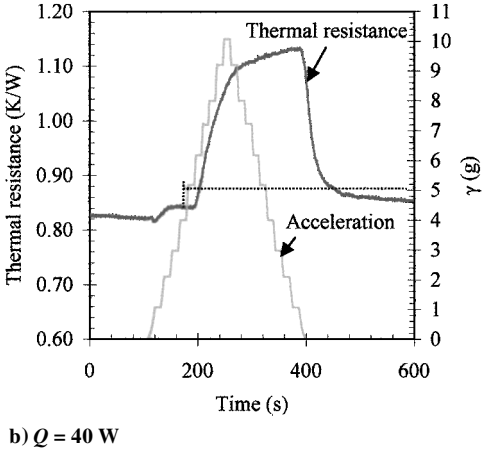

b) Q = 40 W

Fig. 17 Thermal resistance variations vs time (acceleration of type 2).

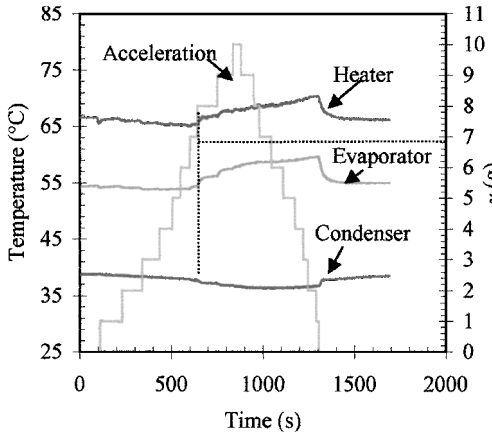

a) Q = 20 W

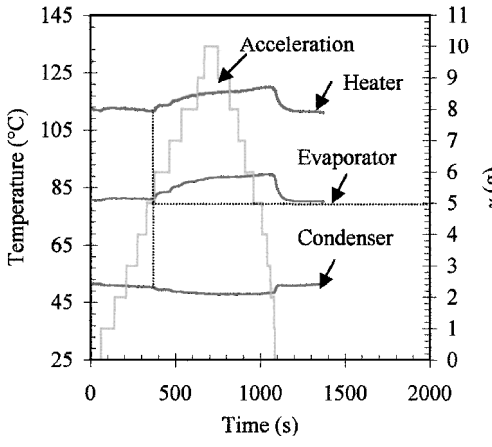

b) Q = 40 W

Fig. 18 Temperature variations vs time (acceleration of type 3).

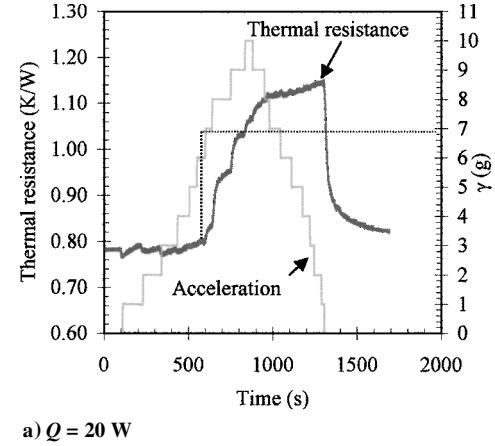

a) Q = 20 W

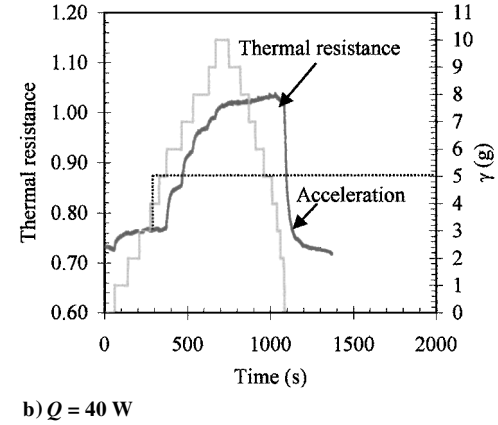

b) Q = 40 W

Fig. 19 Thermal resistance variations vs time (acceleration of type 3).

$Q = 20$ W (Fig. 19a) and 60% for $Q = 40$ W (Fig. 19b) for 10-g acceleration level.

Discussion

When subjected to axial unfavorable acceleration, a redistribution of the working fluid within the capillary structure occurs. The excess working fluid is pooled into the condenser section. This is evidenced by the decrease in condenser temperature with a subsequent increase in acceleration (Figs. 14, 16, and 18). This pooling, which is a direct result of the mounting configuration of the heat pipe on the centrifuge table, reduces the effective condensation area implying that there should be an increase in the evaporator temperature, which occurs for a certain critical level of the acceleration depending on the input heat load as it is given in Table 5. Onset of dryout occurs with evaporator temperature increase. For this case a subsequent reduction in the acceleration, while maintaining power to the heat pipe, has no immediate effect on the operating temperature once dryout has started. This results in a plateau in the operating temperature until there is a sufficient reduction in the acceleration to reprime the heat pipe thereby reducing the operating temperature. This hysteresis, which significantly altered the heat pipe transient behavior once dryout was initiated, can be explained by the rewetting behavior of the capillary structure under different input heat loads and acceleration types.

Indeed, by examining the thermal behavior of the heat pipe under acceleration types 1 and 2, it can be noticed that almost the same behavior is obtained when operating with input heat fluxes less than 30 W, that is, the heat pipe is not repriming when the acceleration is suppressed. However, for $Q = 40$ W a partial repriming of the heat pipe is obtained for acceleration type 1, and a total repriming is observed for acceleration type 2. For the acceleration type 3 a repriming of the heat pipe is observed when the acceleration is suppressed whatever the input heat flux rate. These phenomena can be explained by the effect of the acceleration profile on the liquid distribution within the heat pipe and the hydrodynamics aspects relative to the liquid and vapor flow within the porous capillary structure under acceleration forces.

When operating with low input heat flux rates under zero-field acceleration, the liquid distribution within the heat pipe is such that no blocking liquid is trapped in the condenser, and so all of the liquid charge is circulating within the porous capillary structure. When accelerations of types 1 or 2 are applied, 10-g acceleration level is reached after 94 s and 140 s, respectively, the condenser flooding is abrupt, and a large amount of the circulating liquid is blocked in the condenser section. Because for low heat loads the liquid velocity is weak, the axial acceleration forces are greater than the liquid inertial forces, the repriming of the heat pipe is not immediate after acceleration suppression, and a long time is needed for the heat pipe to reprime. Actually, the repriming of the heat pipe under these conditions is observed when the input heat is suppressed for 15 min and then set to its value before suppression.

For high heat loads approaching dryout under zero acceleration field, liquid flows faster. In these conditions pushing the liquid toward the condenser section under acceleration forces of types 1 or 2 causes a faster dryout in the evaporator section under low acceleration level (see Table 5). However, the repriming of the heat pipe when acceleration is suppressed is immediate because liquid velocity is high.

For acceleration type 3 10-g acceleration level is reached after 900 s. For low as well as high heat fluxes, the redistribution of the liquid within the porous capillary structure after applying acceleration type 3 is not abrupt because a waiting time corresponding to the thermal stabilization operation after each acceleration level increase is imposed. When operating with low heat flux rates, the waiting time results in a low amount of blocking liquid compared to that obtained for accelerations type 1 or 2. This explains the total repriming of the heat pipe for low heat flux rates under this type of acceleration. For high heat fluxes the total repriming of the heat pipe is caused by the high liquid velocities.

To quantify the repriming or the depriming of the heat pipe, the Bond number is used, which is defined as

Table 5 Synthesis of the experimental results

Acceleration	Type 1			Type 2		Type 3	
Heat input	20	30	40	20	40	20	40
Depriming	6 g	4 g	3 g	5 g	5 g	7 g	5 g
Repriming	No	No	Yes	No	Yes	Yes	Yes
R_{th} increase, %	20	60	70	30	40	50	60

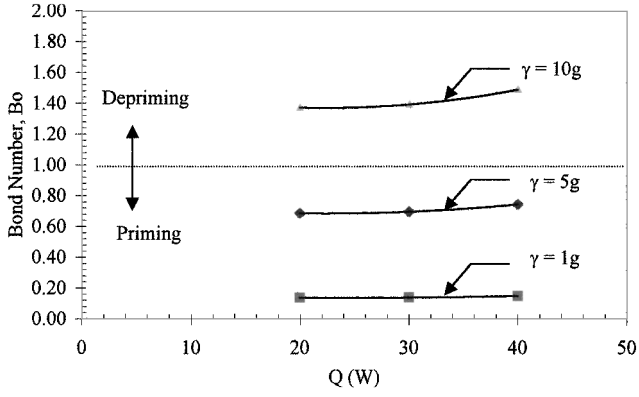

Fig. 20 Bond number variations vs input heat flux rate.

$$Bo = \rho\gamma L d_p / 4\sigma \tag{3}$$

where L is the length of the heat transfer section of the heat pipe and d_p is the average pore diameter. It is clear that the heat-pipe depriming condition holds when the acceleration forces overcome the surface tension forces, that is, $Bo > 1$. For the heat pipe tested in this study, the mean diameter of the pores, which is measured by an electronic microscope, is 250 μm. The liquid density as well as the surface tension are calculated by considering the adiabatic temperature, which is measured for each input heat flux rate.

The Bond number variations as a function of the input heat flux rate are shown in Fig. 20 for different acceleration levels. Note that for a given acceleration Bo increases with increasing input heat flux rate Q. For a given input heat flux rate, Bo increases with increasing acceleration. For $Q = 20$ W, $Bo > 1$, that is, depriming of the heat pipe happens for $\gamma \approx 6$ g. For $Q = 40$ W the heat-pipe depriming happens for 5.5 g. These values are of the same order of magnitude of those determined experimentally under certain acceleration conditions (Table 5). However, estimating the acceleration level, which causes the heat-pipe depriming on the basis of the Bond number considerations, does not take into account the effect of the acceleration type or profile.

From Eq. (3) one can predict the effects of some parameters on the heat-pipe operation under acceleration forces. Among them we distinguish the heat-pipe length and the pore diameter of the capillary structure. Increasing the heat-pipe length results in the depriming of the heat pipe under low acceleration levels. This effect is observed during our experimental tests on other heat-pipe prototypes having different lengths. Indeed, considering longer heat pipes implies more liquid fill charge, and consequently the effect of acceleration is more pronounced. Moreover, reducing the diameter of the pores results in the heat-pipe depriming under high acceleration levels. This trend is evidenced experimentally by Ponnappan et al.[2] who carried out experiments on two porous capillary structures with pore diameters of 55.4 and 306 μm, respectively (Fig. 2).

Conclusions

An investigation into the effects of body forces with constant input heat loads on the performance of flat copper heat pipe has been conducted. The heat-pipe thermal performance is hardly affected by gravitational and vibration forces. Transient acceleration forces are generated to simulate acceleration forces for high-performance aircraft maneuvering in amplitude, duration, and direction. Pooling of the excess working fluid plays a significant role in the heat transport potential of the heat pipe subjected to accelerations. There

is a decrease in the heat-pipe thermal performance with increasing acceleration as a result of partial dryout of the evaporator and pooling in the condenser. Dryout, which is demonstrated as a result of increased acceleration, depends on the input heat power and the acceleration profile. However, under certain conditions the heat pipe successfully reprimed for high continuous input heat load, with a suppression of acceleration. In all cases the increase of the heat-pipe thermal resistance does not exceed 70%. The maximum heat-pipe thermal resistance obtained under 10-*g* acceleration level is about 1.1 K/W, which remains an acceptable value for the electronic package safety.

This investigation has demonstrated the potential use of heat-pipe technology in a transient body force environment. However, characteristic timescales for constant heat loads, coupled body force effects, and transient accelerations will define the transient or steady performance of the heat pipe.

The next step of this work will be the study of the effects of steady periodic cycle and burst cycle radial acceleration forces on the transient heat-pipe thermal performance.

Acknowledgments

This work was supported in part by Sextant Avionique, Valence, France. The first author would like to acknowledge the technical and financial supports provided by the Industrial System Department. Special thanks go to C. Sarno, Head of the Electronic Packaging Division, for his permanent assistance and guidance.

References

[1]Kiseev, V. M., Belonogov, A. G., and Belyaev, A. A., "Influence of Adverse Accelerations on the Operation of an Antigravity Heat Pipe," *Journal of Engineering Physics*, Vol. 50, 1986, pp. 394–398.

[2]Ponnappan, R., Yerkes, K. L., Chang, W. S., and Beam, J. E., "Analysis and Testing of Heat Pipe in Accelerating Environment," *Proceedings 8th International Heat Pipe Conference*, 1992, pp. B-19-1–B-19-6.

[3]Yerkes, K. L., and Beam, J. E., "Arterial Heat Pipe Performance in a Transient Heat Flux and Body Force Environment," Society of Automotive Engineers, Paper 921944, Oct. 1992.

[4]Peng, X. F., and Peterson, G. P., "Acceleration-Induced Depriming of External Artery Heat Pipes," *Journal of Thermophysics and Heat Transfer*, Vol. 6, No. 3, 1992, pp. 546–549.

[5]Ochterbeck, J. M., Peterson, G. P., and Ungar, E. K., "Depriming/Rewetting of Arterial Heat Pipes: Comparison with Share-II Flight Experiment," *Journal of Thermophysics and Heat Transfer*, Vol. 9, No. 1, 1995, pp. 101–108.

[6]Thomas, S., and Yerkes, K., "Quasi-Steady State Performance of a Heat Pipe Subjected to Transient Acceleration Loadings," *Journal of Thermophysics and Heat Transfer*, Vol. 11, No. 3, 1997, pp. 306–309.

[7]Romestant, C., and Alexander, A., "Performances of Heat Pipes Under High Acceleration Field," *Proceedings of the 10th IHPC Conference*, 1997.

[8]Thomas, S. K., Klasing, K. S., and Yerkes, K. L., "The Effects of Transverse Acceleration-Induced Body Forces on the Capillary Limit of Helically Grooved Heat Pipes," *Journal of Heat Transfer*, Vol. 120, May 1998, pp. 441–450.

[9]Deverall, J. E., "The Effect of Vibration on Heat Pipe Performance," Los Alamos National Lab., Rept. LA-3798, Los Alamos, NM, Nov. 1967.

[10]Richardson, J. W., Whitehurst, C. A., and Whitehouse, G. D., "The Effect of Longitudinal Vibration on Heat Pipe Performance," *Journal of Astronautical Sciences*, Vol. 17, No. 2, 1970, pp. 249–266.

[11]Peterson, G. P., *An Introduction to Heat Pipes,* 1st ed., Wiley, New York, 1994.

[12]Faghri, A., *Heat Pipe Science and Technology*, 1st ed., Taylor and Francis, Washington, DC, 1995.

[13]Kline, S. J., and McClintock, F. A., "The Description of Uncertainties in Single Sample Experiments," *Mechanical Engineering*, Vol. 75, Jan. 1953, pp. 3–9.